

# Brain Atlas-based Lesion Spatial Distribution and Modeling of Wallerian Degeneration In Multiple Sclerosis

K. M. Hasan<sup>1</sup>, I. S. Walimuni<sup>1</sup>, S. Datta<sup>1</sup>, F. Nelson<sup>2</sup>, J. S. Wolinsky<sup>3</sup>, and P. A. Narayana<sup>4</sup>

<sup>1</sup>Radiology, UTHSCH, Houston, Texas, United States, <sup>2</sup>Neurology, UTHSCH, Houston, Texas, <sup>3</sup>Neurology, UTHSCH, Houston, Texas, United States, <sup>4</sup>Radiology, UTHSCH, Houston, Uexasa, United States

**Introduction:** Wallerian degeneration (WD) of axons proximal to inflammatory lesions in multiple sclerosis (MS) has been proposed as one contributor to quantitative MRI (qMRI) abnormalities detected in normal-appearing gray matter (NAGM) and white matter (NAWM) [1, 2]. The literature on the role of lesions and their impact on qMRI metrics of normal brain tissue is contradictory [4-7]. The availability of a detailed tabulation of the spatial distribution of lesions in a standardized human brain atlas of deep subcortical, cortical gray matter and white matter lobes and fiber tracts will help model the effect of lesions on regional qMRI metrics derived using multi-modal MRI methods [8]. In this work, we describe a computational framework that provides human brain atlas-based regional lesion volume, NAWM and NAGM volumetry and their corresponding microstructural qMRI metrics (e.g. relaxation, anisotropy, axial, radial and mean diffusivities). We applied our methods to provide lesion distribution maps of a cohort of relapsing remitting (RR) MS patients relative to anatomical labels of deep GM nuclei, cortical GM matter parcellation and white matter tracts [9] provided by the international consortium for brain mapping (ICBM) [10, 11] and **FreeSurfer** [12]. We demonstrate the importance of lesion volume distribution and proximity to explain disability in MS.

**Methods: Subjects:** We included 87 **RRMS patients** (77% females; age = 42.6±9.9 years), disease duration (DD) = 11.0±2.8 years, extended disability status score (EDSS) = 1.7±1.6 (range=0-6.5) and total lesion load or burden of disease (BOD) = 12.3±11.7 mL (see **Figure 1** below). **Conventional MRI Acquisition:** MRI studies were performed on a 3T Philips Intera scanner with a dual quasar gradient system and an eight channel SENSE-compatible head coil. The MRI protocol included a T1-weighted 3D-SPGR with isotropic voxel size = 0.9375 mm for tissue volumetry, dual fast spin-echo (FSE; TE<sub>1</sub>/TE<sub>2</sub>/TR = 11/90/6800), fluid-attenuated inversion recovery (FLAIR; TE/TR = 80/2500/80) for lesion segmentation [8]. **Data Processing:** All MRI data sets were masked to remove non-brain tissues and the intracranial volume (ICV) was computed. MS lesions were segmented using the DSE and FLAIR data as described elsewhere [8]. Tissue volumes were obtained by the application of T2-weighted atlas-based methods on the lesion demodulated T2-weighted data [11] and **FreeSurfer** on the T1-weighted volume [12]. Lesion spatial distribution or probability map was computed using SPM as described elsewhere [3-6,11,13,14]. All volumes (dual-echo, derived lesion masks and qMRI microstructural maps) were registered with T1-weighted data where regions are labeled using standardized ICBM [10] and **FreeSurfer** atlases [12]. The **FreeSurfer** brain volumes demodulated by the lesion masks were used to obtain the regional qMRI average values for all atlas labels. **Atlas-based Anatomical Labels:** The brain atlas covered the frontal, temporal, parietal, occipital, cingulate and insular cortices and corresponding white matter analogue. The deep GM tissue included the putamen, globus pallidus, hippocampus, amygdale and accumbens. The corpus callosum (CC) subdivisions, insular white matter were also included. Further, we have used the DTI-81 white matter tractography atlas [9,10] in standard space to compute the frequency that lesions intercepted an anatomical label assigned to a host of commissural (e.g. CC), association (e.g. uncinate, inferior and superior longitudinal fasciculus), projection (e.g. corona radiata, corticospinal tract) and limbic pathways (e.g. cingulum, fornix) as described in Wakana et al. [9]. **Validation of Volumetry and Lesion Maps:** Our automated lesion distribution results were validated using a trained physician who tabulated lesion frequency on all patients. The volumetry results on MS patients were compared with those obtained on healthy controls. **Statistical Analysis:** Correlations between age, EDSS, DD and regional metrics were computed using the Pearson correlation or Spearman coefficients.

**Results:** **Figure 1** shows the scatter and linear correlations between EDSS, DD, BOD and age on our RRMS cohort. As expected, EDSS increased with BOD and DD [15]. Representative lesion maps on our RRMS cohort using the ICBM, DTI-81 and **FreeSurfer** atlases are shown in **Fig. 2** and **Fig. 3** where lesions are assigned a **hot-red color**. The volume of lesions and frequency in brain atlas labels (e.g. nuclei, tracts, cortex, sub-lobar) were extensively tabulated (*only a summary is provided here*). Note that lesions in cortical GM are less frequent than subcortical GM regions. Lesions in WM are more frequent than those in GM (e.g. insular GM ~ 35%; insular WM 50%). Lesions in the hippocampus are more frequent (~65%) than in the amygdale (20%). Lesions in the caudate (100%) are more frequent than those in the putamen (10%), and lesions in the thalamus GM are *least frequent* in our cohort (~15%). As depicted in **Fig. 3**, lesions in the parietal and occipital lobes WM are dominantly intercepting the corona radiata and optic radiations. As one important representative of the quantitative results, **Figure 4** shows a scatter plot of the regional lesion volume in the corona radiata and its significant correlation with (A) EDSS and (B) DD (compare **Fig. 4** & **Fig. 1** using the entire brain BOD). **Discussion:** To our knowledge, this is the first report on RRMS brain spatial distribution of lesions using the ICBM and **FreeSurfer** gray and white matter atlases that included fiber pathways. Our results on the topology (**Fig. 2, 3**), subcortical and lobar distribution of lesions in gray and white matter are consistent with a *postmortem* histopathology report by Brownwell B and Hughes in 1962 [16]. The significant correlation between regional lesion volume of the corona radiata with EDSS and DD show the importance of regional lesion mapping as applied to brain function at the system-level and warrant the examination of serial data and different MS phenotypes.

**References:** [1] Filippi M, Agosta F. JMRI. 2010;31:770-88 [2] Charil A et al. Neuroimage 2003;19:532-44 [3] Narayanan S et al. Ann Neurol 1997;41:385-91 [4] Vellinga MM et al. J Magn Reson Imaging 2009;29:768-73 [5] Bodini et al. JNNP 2010 (*in press*) [6] Kezle TB et al. Mult Scler. 2008;14:779-85 [7] Antulov et al. J Neuroimaging 2010 (*in press*) [8] Sajja BR et al. Ann Biomed Eng 2006;34:142-51 [9] Wakana et al. Radiology. 2004;230:77-87 [10] Mori S et al. Neuroimage. 2008;40:570-82 [11] Hasan KM et al. Magn Reson Med 64:1382-9 [12] Fischl B et al. Neuron. 2002;33:341-55 [13] Zijdenbos AP et al. IEEE TMI. 2002;21:1280-91 [14] Sepulcre J et al. Neuroimage. 2008;42:1237-43 [15] Trojano M et al. Ann Neurol. 2002;51(4):475-80 [16] Brownwell B and Hughes JT. JNNP 1962;25:315-20.

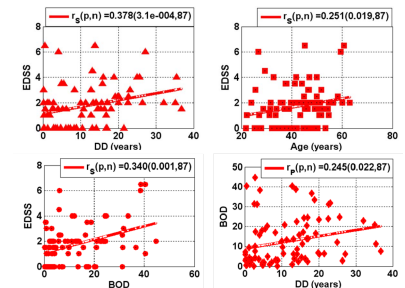


**Fig. 1** RRMS population clinical info.

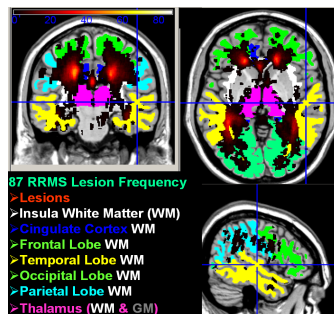


**Figure 2.** Lesion map using **FreeSurfer**.

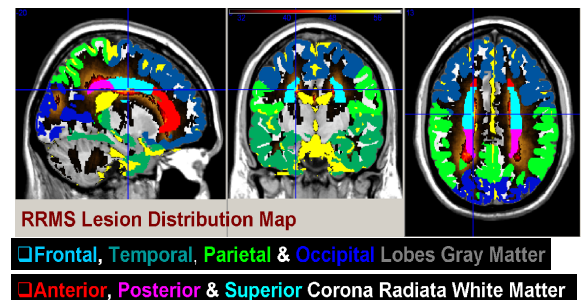


**Figure 3.** Lesion map using ICBM and DTI-81 atlas.

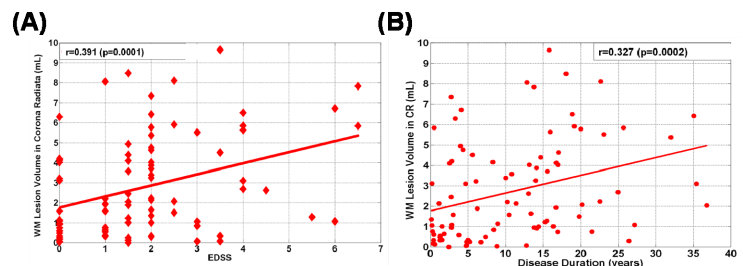


**Figure 4.** Corona Radiata total lesion volume vs. EDSS and DD.